Demonstration Data Report

EMI Array for Cued UXO Discrimination
Demonstration Data Report
Former Camp San Luis Obispo
TEMADS Cued Survey

MAY 2010

Glenn R. Harbaugh
Daniel A. Steinhurst
Nova

David C. George
G&G

James B. Kingdon
Dean K. Keiswetter
Thomas H. Bell
SAIC

Approved for public release; distribution unlimited.

Environmental Security Technology Certification Program

Contents

Figures vi

Tables viii

Acronyms ix

1.0 Introduction 1

1.1 Organization of this document 1

1.2 Study Background and Objectives 1

1.3 Specific Objectives of Demonstration 1

2.0 Technology 1

2.1 Technology Description 1

2.1.1 EMI Sensors 1

2.1.2 Sensor Array 5

2.1.3 Application of the Technology 9

2.1.4 Development of the Technology 9

2.2 Advantages and Limitations of the Technology 12

3.0 Performance Objectives 12

3.1 Objective: Site Coverage 13

3.1.1 Metric 14

3.1.2 Data Requirements 14

3.1.3 Success Criteria 14

3.2 Objective: Calibration Strip Results 14

3.2.1 Metric 14

3.2.2 Data Requirements 14

3.2.3 Success Criteria 14

3.3 Objective: Location Accuracy 14
3.3.1 Metric 15
3.3.2 Data Requirements 15
3.3.3 Success Criteria 15
3.4 Objective: Depth Accuracy 15
3.4.1 Metric 15
3.4.2 Data Requirements 15
3.4.3 Success Criteria 15
3.5 Objective: Production Rate 15
3.5.1 Metric 16
3.5.2 Data Requirements 16
3.5.3 Success Criteria 16
3.6 Objective: Data Throughput 16
3.6.1 Metric 16
3.6.2 Data Requirements 16
3.6.3 Success Criteria 16
3.7 Objective: Reliability and Robustness 16
3.7.1 Data Requirements 17
4.0 Site Description 17
5.0 Test Design 17
5.1 Conceptual Experimental Design 17
5.2 Site Preparation 17
5.3 Systems Specification 17
5.3.1 MTADS Tow Vehicle 17

5.3.2 RTK GPS System 18
5.3.3 Time-Domain Electromagnetic Sensor 18
5.4 Calibration Activities 19
5.4.1 TEMTADS Sensor Calibration 19
5.4.2 Emplaced Sensor Calibration Items 19
5.5 Data Collection Procedures 20
5.5.1 Scale of Demonstration 20
5.5.2 Sample Density 20
5.5.3 Quality Checks 20
5.5.4 Data Handling 21
5.6 Validation 21
6.0 Data Analysis Plan 21
6.1 Preprocessing 21
6.2 Parameter Estimation 22
6.3 Data Product Specifications 23
7.0 performance results 24
7.1 Objective: Site Coverage 25
7.1.1 Metric 25
7.1.2 Data Requirements 26
7.1.3 Success Criteria 26
7.1.4 Results 26
7.2 Objective: Calibration Strip Results 26
7.2.1 Metric 26
7.2.2 Data Requirements 26

7.2.3 Success Criteria 26
7.2.4 Results 27
7.3 Objective: Location Accuracy 30
7.3.1 Metric 30
7.3.2 Data Requirements 30
7.3.3 Success Criteria 31
7.3.4 Results 31
7.4 Objective: Depth Accuracy 31
7.4.1 Metric 31
7.4.2 Data Requirements 31
7.4.3 Success Criteria 31
7.4.4 Results 31
7.5 Objective: Production Rate 31
7.5.1 Metric 31
7.5.2 Data Requirements 32
7.5.3 Success Criteria 32
7.5.4 Results 32
7.6 Objective: Data Throughput 32
7.6.1 Metric 32
7.6.2 Data Requirements 32
7.6.3 Success Criteria 32
7.6.4 Results 33
7.7 Objective: Reliability and Robustness 33
7.7.1 Data Requirements 33

7.7.2 Results 33

8.0 Schedule of Activities 34

9.0 Management and Staffing 34

10.0 References 35

Appendix A. Points of Contact A-1

Appendix B. Data Formats B-1

B.1 Position / orientation data file (*.GPS) B-1

B.2 TEM Data file (*.TEM) B-1

B.3 Anomaly Parameter Output file B-2

Figures

Figure 2-1 – Construction details of an individual EMI sensor (left panel) and the assembled sensor with end caps attached (right panel). 2

Figure 2-2 – Measured transmit current (upper panel), full measured signal decay (middle panel), and gated decay (lower panel) as discussed in the text. 3

Figure 2-3 – Measured response from a 2-in steel sphere 25 cm from the sensor. Decays 1, 1001, 2001, and 3001 from a series that started from a cold start are plotted along with the expected response from this target. 4

Figure 2-4 – Measured response from three calibration coils and the background response between measurements plotted on a semi-log plot to emphasize the exponential nature of the decay. The decay time constants extracted from the measurements are listed in the legend. 4

Figure 2-5 – Sketch of the EMI sensor array showing the position of the 25 sensors and the three GPS antennae. 5

Figure 2-6 – Sensor array mounted on the MTADS EMI sensor platform. 6

Figure 2-7 – Comparison of the response of the array members. The measured decay from a 2-in steel sphere held 30 cm below each sensor in turn is plotted. The decays are indistinguishable. 6

Figure 2-8 – The response of nine of the individual sensors to a 40-mm projectile located under the center of the array. 7

Figure 2-9 – Derived response coefficients for a 40-mm projectile using the measurements of which the decays shown in Figure 2-8 are a subset. 8

Figure 2-10 – Derived response coefficients from a cued measurement over "Cylinder E" in the test field. 8

Figure 2-11 – Three sets of βs derived from three measurements over a 4.2-in mortar baseplate at different position/orientation pairs. 9

Figure 5-1 – MTADS tow vehicle and magnetometer array. 18

Figure 6-1 – Principal axis polarizabilities for a ½ cm thick by 25cm long by 15cm wide mortar fragment. 23

Figure 7-1 – Peak signals compared with response curve for a 2.36-in rocket. 28

Figure 7-2 – Peak signals compared with response curve for a 4.2-in mortar.....28

Figure 7-3 – Peak signals compared with response curve for a 60-mm mortar. 29

Figure 7-4 – Peak signals compared with response curve for an 81-mm mortar. 29

Figure 8-1 – Schedule of all demonstration activities including deliverables. 34

Figure 9-1 – Management and Staffing Wiring Diagram. 34

Tables

Table 2-1 – TEMTADS Blind Grid Test Area P_d^{disc} Results 11

Table 2-2 – TEMTADS Blind Grid Test Area P_{fp}^{disc} Results 11

Table 2-3 – TEMTADS Indirect Fire Test Area P_d^{disc} Results 11

Table 2-4 – TEMTADS Indirect Fire Test Area P_{fp}^{disc} Results 11

Table 2-5 – TEMTADS Blind Grid Test Area Efficiency and Rejection Rates 12

Table 2-6 – TEMTADS Indirect Fire Test Area Efficiency and Rejection Rates 12

Table 3-1 – Performance Objectives for This Demonstration 13

Table 7-1 – Details of Former Camp SLO Calibration Strip 24

Table 7-2 – Performance Objectives for This Demonstration 25

Table 7-3– Peak Signals for Calibration Strip Emplaced Items 27

Table 7-4 – Position Accuracy and Variability for Calibration Strip Emplaced Items 30

Acronyms

Abbreviation	Definition
AMTADS	Airborne Multi-sensor Towed Array Detection System
APG	Aberdeen Proving Ground
ASCII	American Standard Code for Information Interchange
ATC	Aberdeen Test Center
CD-R	Compact Disk - Recordable
DAQ	Data Acquisition (System)
DAS	Data Analysis System
DVD-R	Writable digital versatile disc
EMI	Electro-Magnetic Induction
ESTCP	Environmental Security Technology Certification Program
FQ	Fix Quality
FUDS	Formerly -Used Defense Site
GPS	Global Positioning System
HASP	Health and Safety Plan
Hz	Hertz
MM	Munitions Management
MTADS	Multi-sensor Towed Array Detection System
NMEA	National Marine Electronics Association
NRL	Naval Research Laboratory
Pd	Probability of Detection
POC	Point of Contact
(PTNL,)AVR	Time, Yaw, Tilt, Range for Moving Baseline RTK NMEA-0183 message
(PTNL,)GGK	Time, Position, Position Type, DOP NMEA-0183 message
QC	Quality Control
ROC	Receiver Operating Characteristic
RTK	Real Time Kinematic
Rx	Receiver
SAIC	Science Applications International Corporation
SERDP	Strategic Environmental Research and Development Program
SLO	San Luis Obispo
TEM	Time-domain Electro-Magnetic
TEMTADS	Time-domain Electro-Magnetic MTADS
Tx	Transmit(ter)
UXO	Unexploded Ordnance

1.0 INTRODUCTION

1.1 ORGANIZATION OF THIS DOCUMENT

The data collection report for the Multi-sensor Towed Array Detection System (MTADS) EMI Array for Cued Discrimination, or TEMTADS, for participation in the Environmental Security Technology Certification Program (ESTCP) UXO Classification Study at former Camp San Luis Obispo (Camp SLO), CA in 2008-2009, is presented in this document. To limit the repetition of the information, Study- and site- specific information that is presented elsewhere, either in the ESTCP UXO Classification Study Demonstration Plan or the MTADS Magnetometer / EM61 MKII Demonstration Plan [1], are noted and not repeated in this document.

1.2 STUDY BACKGROUND AND OBJECTIVES

Please refer to the ESTCP UXO Classification Study Demonstration Plan.

1.3 SPECIFIC OBJECTIVES OF DEMONSTRATION

As part of the ESTCP UXO Classification Study, Nova Research, Incorporated and SAIC conducted a cued discrimination survey within the 11.8 acre demonstration site at the Former Camp SLO, CA. This survey was conducted using the Naval Research Laboratory (NRL) TEMTADS. Characterization of the system responses to the items of interest was determined using on site measurements from the Calibration Strip. These data were collected in accordance with the overall study objectives and demonstration plan. This document describes the TEMTADS data collection effort at the former Camp SLO.

2.0 TECHNOLOGY

2.1 TECHNOLOGY DESCRIPTION

2.1.1 EMI Sensors

The EMI sensor used in the TEMTADS array is based on the Navy-funded Advanced Ordnance Locator (AOL), developed by G&G Sciences. The AOL consists of three transmit coils arranged in a 1-m cube; we have adopted the transmit (Tx) and receive (Rx) subsystems of this sensor directly, converted to a 5 x 5 array of 35 cm sensors, and made minor modifications to the control and data acquisition computer to make it compatible with our deployment scheme.

A photograph of an individual sensor element under construction is shown in the left panel of Figure 2-1. The transmit coil is wound around the outer portion of the form and is 35 cm on a side. The 25-cm receive coil is wound around the inner part of the form which is re-inserted into the outer portion. An assembled sensor with the top and bottom caps used to locate the sensor in the array is shown in the right panel of Figure 2-1.

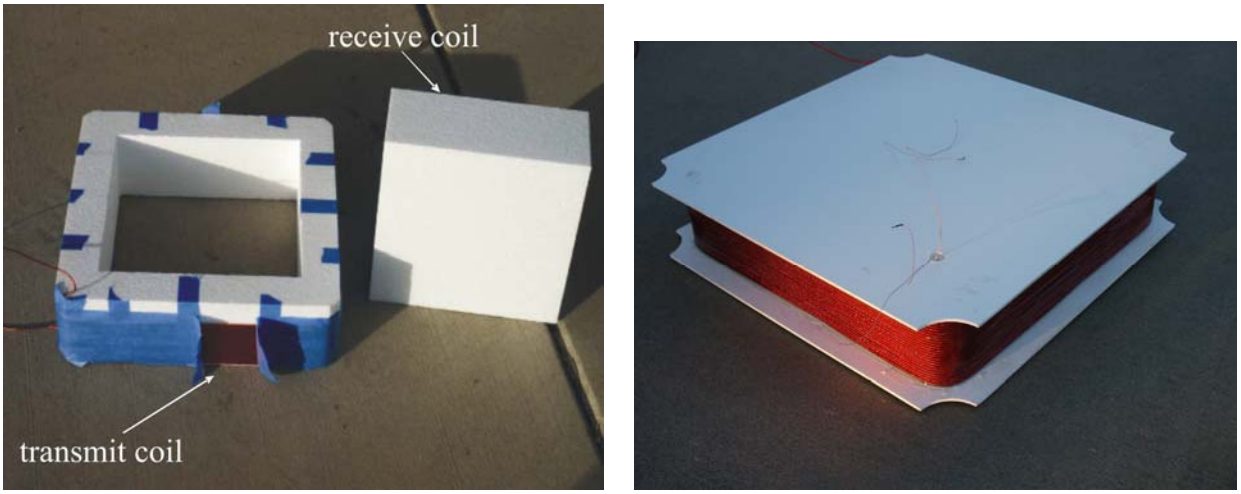

Figure 2-1 – Construction details of an individual EMI sensor (left panel) and the assembled sensor with end caps attached (right panel).

Decay data were collected with a 500 kHz sample rate until 25ms after turn off of the excitation pulse. This results in a raw decay of 12,500 points, which is too many to be practical. These raw decay measurements are grouped into 115 logarithmically-spaced "gates" whose center times range from 42 μs to 24.35 ms with 5% widths and are saved to disk. An example of the measured transmit pulse, raw decay, and gated decay is shown in Figure 2-2.

The individual sensors (consisting of transmit electronics, transmit and receive coils, pre-amp, and digitizer) were characterized at G & G Sciences. Examples of the characterization data are shown in Figure 2-3 and Figure 2-4. System stability is shown in Figure 2-3 which plots the normalized (by measured transmit current) response of a 2 in steel ball at 25 cm separation from the sensor. The data plotted are decays 1, 1001, 2001, and 3001 in a continuously-triggered series that began from a cold start and ran for 2.5 hours. For comparison purposes, the expected response from this sphere is plotted in black. As can be seen, the sensor exhibits excellent stability.

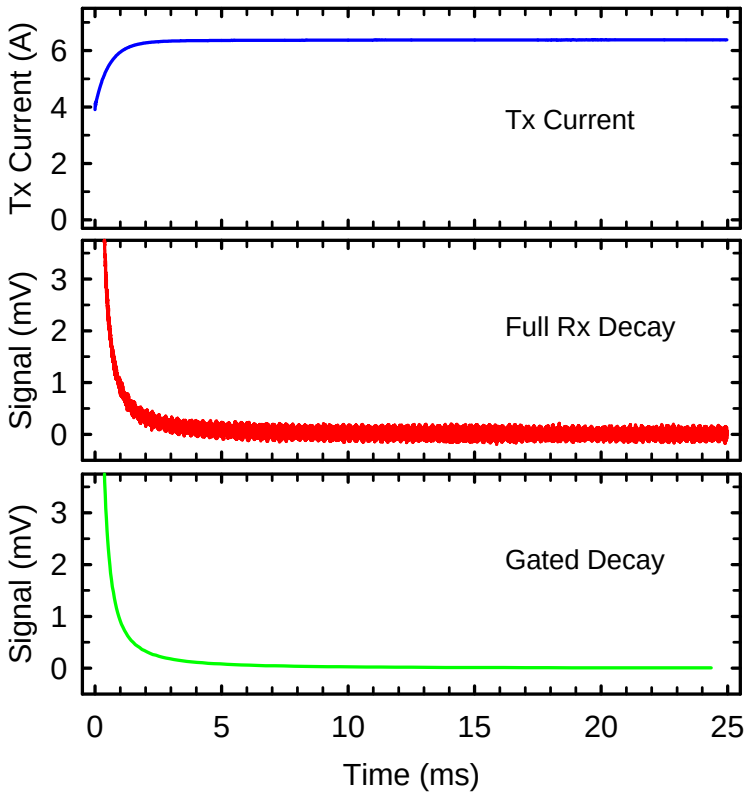

Figure 2-2 – Measured transmit current (upper panel), full measured signal decay (middle panel), and gated decay (lower panel) as discussed in the text.

Because we typically collect decay data to late times and over several orders of magnitude in amplitude, the linearity of system response is very important. To characterize this property of the sensor, we constructed a series of copper coils with nominal decay time constants of 2, 4, and 6 ms. The response of the three coils is shown in Figure 2-4 which displays the measured decay in a semi-log plot. After a transient at early times, the decays exhibit clean exponential behavior with measured decay times of 1.8, 3.3, and 5.8 ms. Careful calculation of the expected decay times at the temperature at which the tests were conducted results in expected values of 1.82, 3.26, and 5.73 ms.

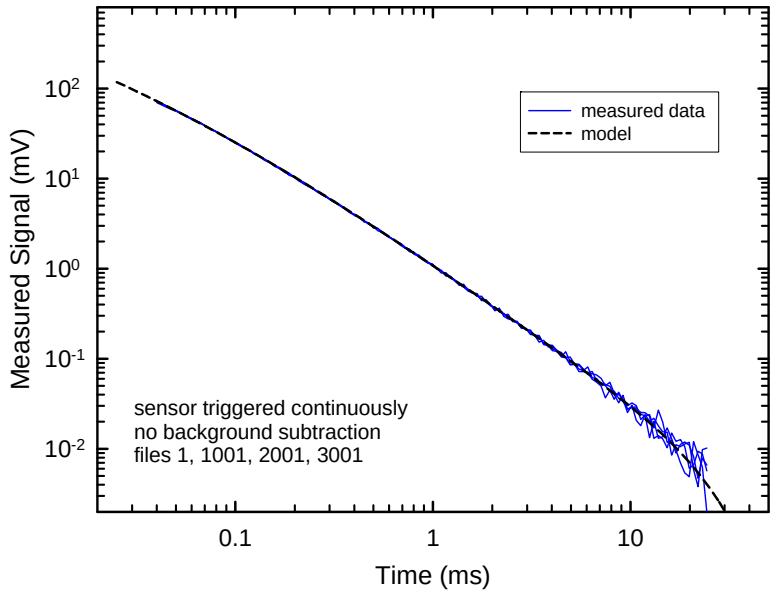

Figure 2-3 – Measured response from a 2-in steel sphere 25 cm from the sensor. Decays 1, 1001, 2001, and 3001 from a series that started from a cold start are plotted along with the expected response from this target.

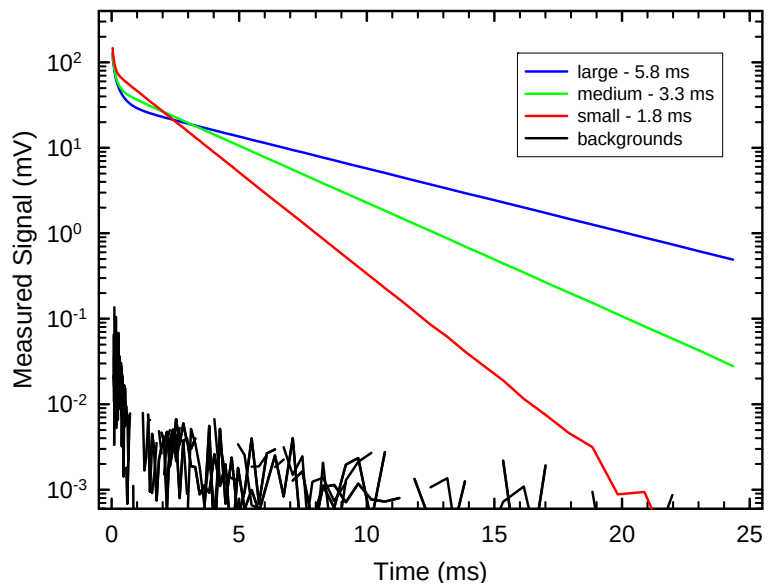

Figure 2-4 – Measured response from three calibration coils and the background response between measurements plotted on a semi-log plot to emphasize the exponential nature of the decay. The decay time constants extracted from the measurements are listed in the legend.

2.1.2 Sensor Array

The twenty-five individual sensors are arranged in a 5 x 5 array as shown in Figure 2-5. The center-to-center distance is 40 cm yielding a 2 m x 2 m array. Also shown in Figure 2-5 is the position of the three GPS antennae that are used to determine the location and orientation of the array for each cued measurement. A picture of the array mounted on the MTADS EMI sensor platform is shown in Figure 2-6.

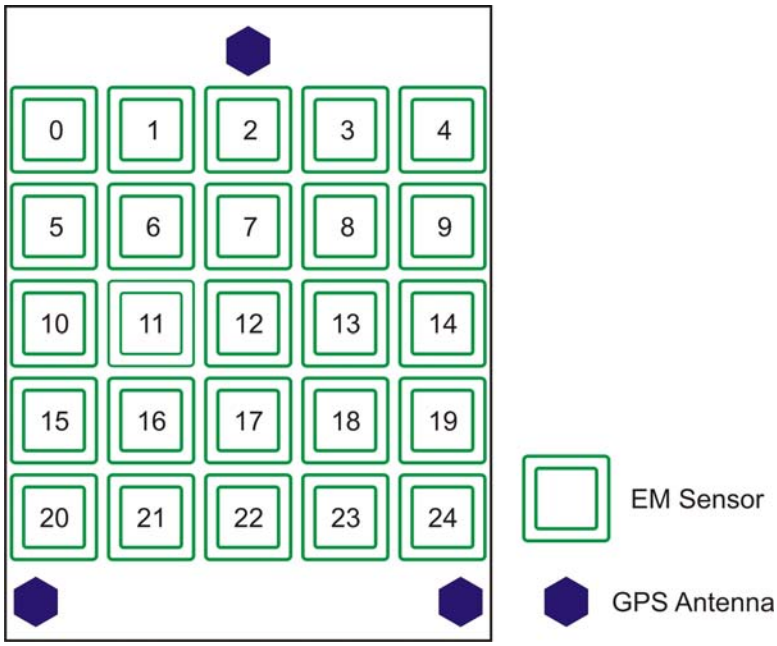

Figure 2-5 – Sketch of the EMI sensor array showing the position of the 25 sensors and the three GPS antennae.

After assembly of the array, a number of array calibration measurements were performed. We first looked at the response for individual sensors. We mounted a two-inch steel sphere 30 cm below each array element in turn. Data collected using this jig are shown in Figure 2-7. As can be seen, the measured decays from each of the sensors plotted are indistinguishable.

After this, the assembled array was used to measure the response of a number of inert ordnance items and simulants both mounted on a test stand and mounted on the sensor platform in our test field. For each series of measurements with the full array, we cycle through the sensors transmitting from each in turn. After each excitation pulse, we record the response of all twenty-five receive coils. Thus, there are 625 (25 x 25) individual transmit/receive pairs recorded, making it difficult to present a full measurement in any coherent way. In Figure 2-8, we plot nine of the transmit/receive pairs resulting from excitation of a 40-mm projectile located under the center of the array. The decays plotted correspond to the signal received on the nine central

sensors (reference Figure 2-5 for the sensor numbering) when that sensor transmits. In other words, the results of nine individual monostatic measurements are presented.

Figure 2-6 – Sensor array mounted on the MTADS EMI sensor platform.

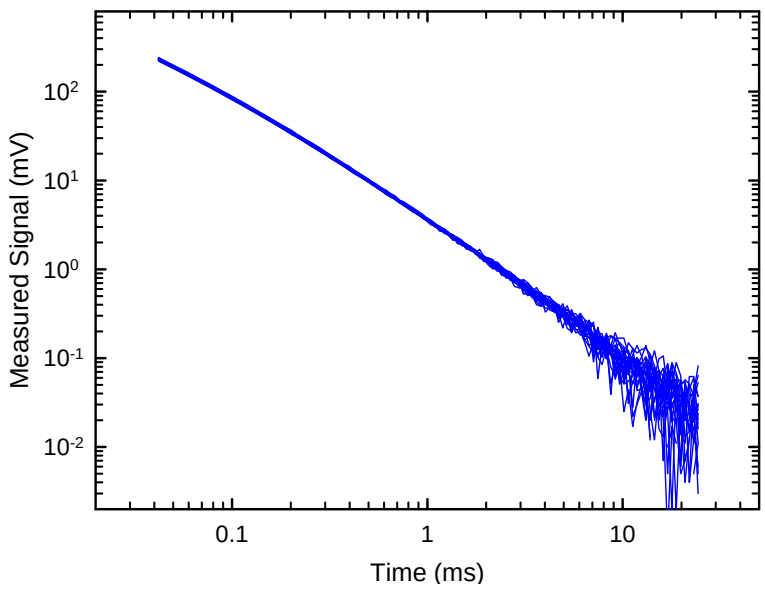

Figure 2-7 – Comparison of the response of the array members. The measured decay from a 2-in steel sphere held 30 cm below each sensor in turn is plotted. The decays are indistinguishable.

All 625 measurements are used for the inversion to recover target parameters. The inversion results for the decay data shown in Figure 2-8 are shown in Figure 2-9. As we expect for an object with axial symmetry such as a 40-mm projectile, we recover one large response coefficient and two equal, but smaller ones. These response coefficients will be the basis of the

discrimination decisions in this demonstration. Derived βs for "Cylinder E" (3" x 12" steel cylinder) in the test field are shown for comparison in Figure 2-10.

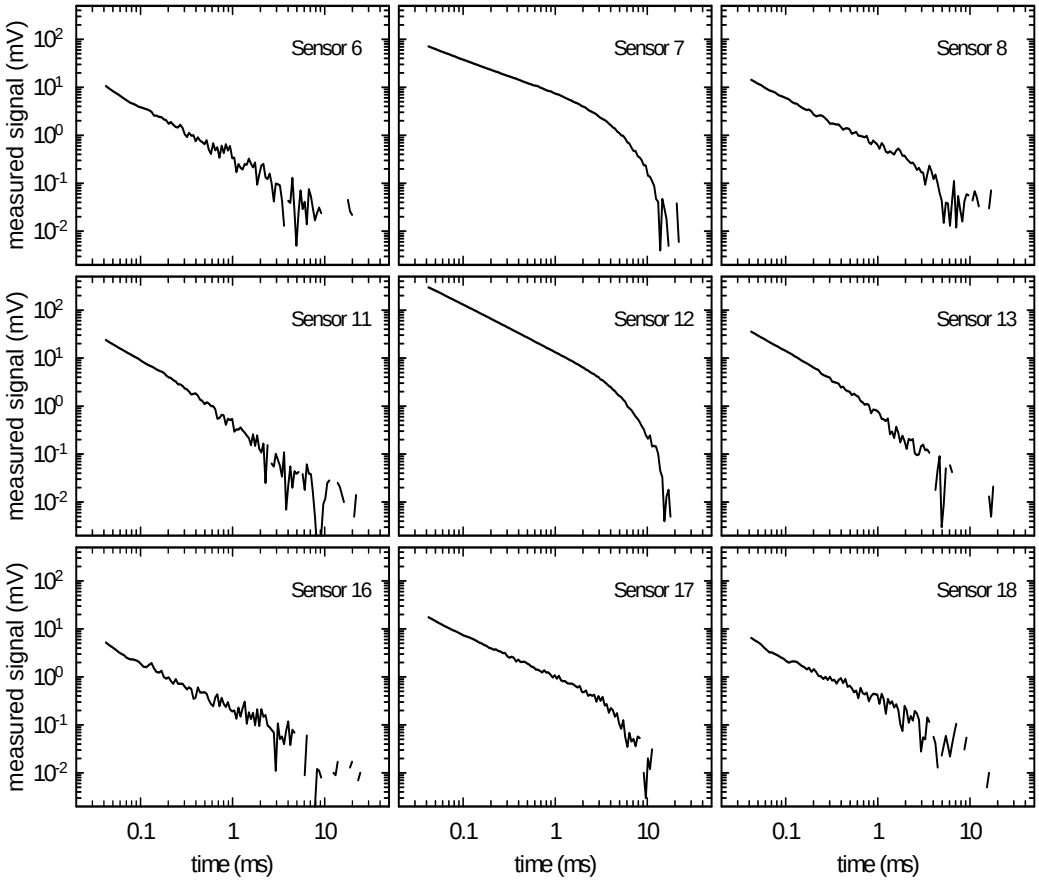

Figure 2-8 – The response of nine of the individual sensors to a 40-mm projectile located under the center of the array.

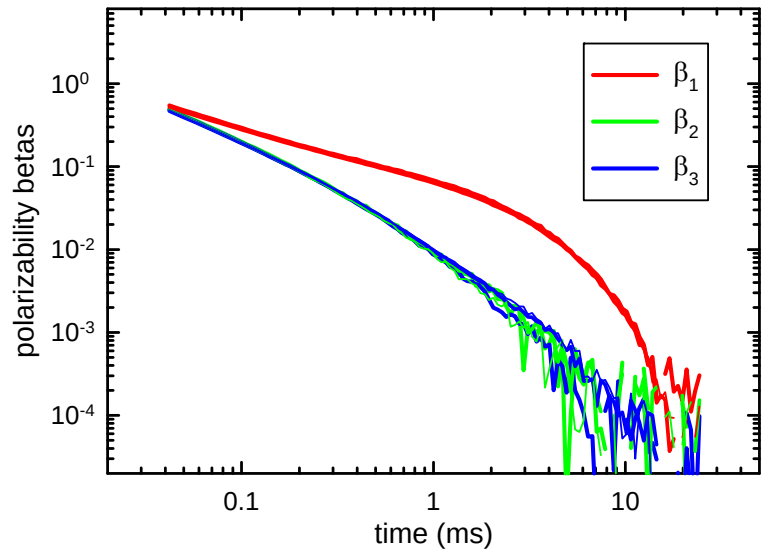

Figure 2-9 – Derived response coefficients for a 40-mm projectile using the measurements of which the decays shown in Figure 2-8 are a subset.

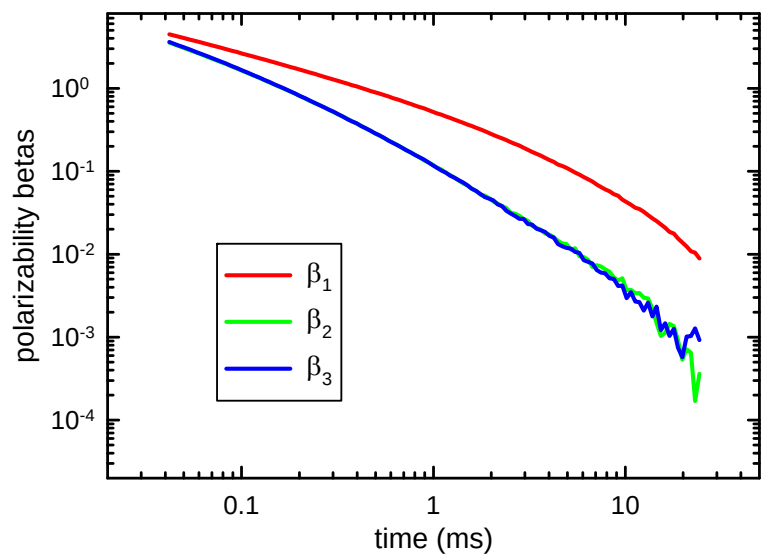

Figure 2-10 – Derived response coefficients from a cued measurement over "Cylinder E" in the test field.

The final array characterization test was to confirm that the response coefficients we recover are invariant to object position and orientation under the array. Figure 2-11 shows the derived βs plotted for a 4.2-in mortar baseplate after measurements at three position/orientation pairs. As can be seen, the inversion results are robust to variation in the object's position and orientation.

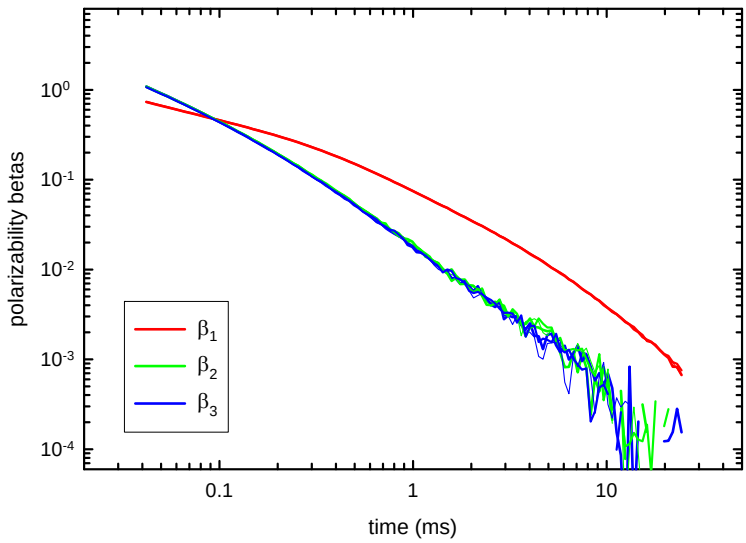

Figure 2-11 – Three sets of βs derived from three measurements over a 4.2-in mortar baseplate at different position/orientation pairs.

2.1.3 Application of the Technology

Application of this technology is straightforward. A list of target positions is developed from some source; in the case of this demonstration, the anomaly list generated from the MTADS EM61 MkII data set. This target file, containing the target location and an optional flag for additional 'stacking' or averaging, is transferred to the system control program which uses the information from the three GPS antennae to guide the operator to position the array over each target in turn. When positioned over the target, we step through the array sensors sequentially, just as in the characterization measurements discussed in the preceding section, and collect decay from all twenty-five receive coils for each excitation. These data are then inverted for target location and characteristics. At the end of the EMI data collection, a few seconds of platform position and orientation data are collected to be used to translate the inverted target position, which is, of course, relative to the array, to absolute position and orientation.

2.1.4 Development of the Technology

The Chemistry Division of the Naval Research Laboratory has participated in several programs funded by SERDP and ESTCP whose goal has been to enhance the discrimination ability of MTADS for both magnetometer and EMI array configurations. The process was based on making use of both the location information inherent in an item's magnetometry response and the shape and size information inherent in the response to the time-domain electromagnetic induction (EMI) sensors that are part of the baseline MTADS in either a cooperative or joint inversion. In these past efforts, our classification ability has been limited by the information available from the time-domain EMI sensor or uncorrected positioning errors.

To make further progress on UXO classification, a sensor with more available information was required. The Geophex, Ltd. GEM-3 sensor is a frequency-domain EMI sensor with up to ten transmit frequencies available for simultaneous measurement of the in-phase and quadrature response of the target. In principle, there will be much more information available from a GEM-3 sensor for use in discrimination decisions. However, the commercial GEM-3 sensor is a hand-held instrument with relatively slow data rates and is thus not very amenable to rapid, wide area surveys. ESTCP Project MM-0033, Enhanced UXO Discrimination Using Frequency-Domain Electromagnetic Induction, was funded to overcome this limitation by integrating an array of GEM-3 sensors with the MTADS platform [2]. Further details can be found in References 2 and 3.

Reference 4 compares the detection-only performance of the magnetometer, the second-generation MTADS EM61 MkII, and the GEMTADS arrays to other demonstrators at both of the Standardized UXO Technology Demonstration Sites. All three sensor arrays were also demonstrated in the Spring of 2007 as part of the ESTCP UXO Discrimination Study at the Former Camp Sibert [3]. Data processing and the development of performance results for the various discrimination methodologies of the UXO Discrimination Study are currently ongoing.

Under SERDP project MM-1315 (EMI Sensor Optimized for UXO Discrimination) and ESTCP project MM-0601, NRL, SAIC, and G&G Sciences have developed a time-domain EMI sensor optimized for the classification of UXO. The TEMTADS array was constructed in 2007 and field tested at the APG Standardized UXO Test Site in June 2008 [5]. For the APG demonstration, a magnetometer data set collected the previous month at the newly reconfigured test site was used for anomaly detection in the manner described in the Magnetometer / MkII Demonstration Plan. Approximately 200 cells in the Blind Grid and 700 anomalies in the Indirect Fire Area were interrogated with the TEMTADS, averaging 200 anomalies/day on the Indirect Fire Area. After processing, ranked dig lists were generated and submitted to ATC for scoring.

The results of the demonstration, as scored by ATC in Reference 5, are briefly summarized here. The TEMTADS surveyed anomalies detected by the MTADS magnetometer system in the Blind Grid and Indirect Fire Areas. For the Blind Grid Test Area, the discrimination stage results are summarized in Table 2-1 and Table 2-2 (subsets of Table 6a of Reference 5), broken out by munitions type and emplacement depth. For the Indirect Fire Test Area, the discrimination stage results are summarized in Table 2-3 and Table 2-4 (subsets of Table 6c of Reference 5), broken out by munitions type and emplacement depth. The Probability of Detection, P_d^{disc}, is defined as the number of discrimination-stage detections / number of emplaced munitions in the test site. The Probability of False Positive, P_{fp}^{disc}, is defined as the (number of discrimination stage false positives)/(number of emplaced clutter items).

Table 2-1 – TEMTADS Blind Grid Test Area P_d^{disc} Results

P_d^{disc}	All Types	105-mm	81/60mm	37/25-mm
Munitions Scores	0.97	0.93	0.97	1.00
0 to 4D	1.00	1.00	1.00	1.00
4D to 8D	1.00	1.00	1.00	1.00
8D to 12D	0.67	0.67	0.00	1.00

Table 2-2 – TEMTADS Blind Grid Test Area P_{fp}^{disc} Results

P_{fp}^{disc}	All Masses	0 to 0.25 kg	>0.25 to 1 kg	>1 to 10 kg
All Depths	0.01	0.02	0.00	0.00
0 to 0.15m	0.01	0.02	0.00	0.00
0.15 to 0.3m	0.00	0.00	0.00	0.00
0.3 to 0.6m	N/A	N/A	N/A	N/A

Table 2-3 – TEMTADS Indirect Fire Test Area P_d^{disc} Results

P_d^{disc}	All Types	105-mm	81/60mm	37/25-mm
Munitions Scores	0.92	0.93	0.93	0.91
By Density				
High	0.88	0.92	0.91	0.80
Medium	0.94	0.97	0.89	0.97
Low	0.94	0.90	0.97	0.94
By Depth				
0 to 4D	0.96	0.94	0.97	0.97
4D to 8D	0.92	0.94	0.92	0.86
8D to 12D	0.72	0.75	0.78	0.67

Table 2-4 – TEMTADS Indirect Fire Test Area P_{fp}^{disc} Results

P_{fp}^{disc}	All Masses	0 to 0.25 kg	>0.25 to 1 kg	>1 to 10 kg
All Depths	0.04	0.03	0.02	0.11
0 to 0.15m	0.04	0.04	0.02	0.13
0.15 to 0.3m	0.04	0.00	0.06	0.06
0.3 to 0.6m	0.08	0.00	0.00	0.20

Efficiency (E) and false positive rejection rate (R_{fp}) are used to score discrimination performance ability at two specific operating points on a ROC curve: one at the point where no decrease in P_d is incurred and the other at the operator-selected threshold. Efficiency is defined as the fraction of detected ordnance correctly classified as ordnance and the false positive rejection rate is defined as the fraction of detected clutter correctly classified as clutter. The results for the Blind

Grid and Indirect Fire Test Areas are summarized in Table 2-5 and Table 2-6, from Tables 7a and 7c of Reference 5.

Table 2-5 – TEMTADS Blind Grid Test Area Efficiency and Rejection Rates

	Efficiency (E)	**False Positive Rejection Rate**
At Operating Point	0.99	0.99
With No Loss of P_d	1.00	0.95

Table 2-6 – TEMTADS Indirect Fire Test Area Efficiency and Rejection Rates

	Efficiency (E)	**False Positive Rejection Rate**
At Operating Point	0.98	0.92
With No Loss of P_d	1.00	0.58

2.2 ADVANTAGES AND LIMITATIONS OF THE TECHNOLOGY

The TEMTADS Array is designed to combine the data advantages of a gridded survey with the coverage efficiencies of a vehicular system. We expect to collect data equal, if not better, in quality to the best gridded surveys (the relative position and orientation of the sensors will be better than gridded data) while interrogating many more targets each field day.

There are limitations to the use of this technology. The array is a 2-m square so fields where the vegetation or topography interferes with passage of that size trailer will not be amenable to the use of the present array. The other serious limitation is anomaly density. For all sensors, there is a limiting anomaly density above which the response of individual targets cannot be separated. We have chosen relatively small sensors for this array which should help with this problem but we cannot eliminate it. Based on experiments at our test pit at Blossom Point, the results of the APG demonstration, and work done on the Camp Sibert data, anomaly densities of 300 anomalies/acre or higher would limit the applicability of this system as more than 20% of the anomalies would have another anomaly within a meter.

3.0 PERFORMANCE OBJECTIVES

Performance objectives for the demonstration are given in Table 3-1 to provide a basis for evaluating the performance and costs of the demonstrated technology. Because this is a classification technology, the performance objectives concentrate on the second step of the UXO survey problem. We assume that the anomalies from all targets of interest have been detected and included on the target list.

Table 3-1 – Performance Objectives for This Demonstration

Performance Objective	Metric	Data Required	Success Criteria
Quantitative Performance Objectives			
Site Coverage	Fraction of assigned anomalies interrogated	Survey results	100% as allowed for by topography / vegetation
Calibration Strip Results	System response consistently matches physics-based model	• System response curves • Daily calibration strip data	• ≤ 15% rms variation in amplitude • Down-track location ± 25cm • All response values fall within bounding curves
Location Accuracy	Average error and standard deviation in both axes for interrogated items	• Estimated location from analyses • Ground truth from validation effort	ΔN and $\Delta E < 5$ cm σN and $\sigma E < 10$ cm
Depth Accuracy	Standard deviation in depth for interrogated items	• Estimated location from analyses • Ground truth from validation effort	ΔDepth < 5 cm σDepth < 10 cm
Production Rate	Number of anomalies investigated each day	• Survey results • Log of field work	125 anomalies/day
Data Throughput	Throughput of data QC process	Log of analysis work	All data QC'ed on site and at pace with survey
Qualitative Performance Objective			
Reliability and Robustness	General Observations	Team feedback and recording of emergent problems	Field team comes to work smiling

3.1 OBJECTIVE: SITE COVERAGE

A list of previously identified anomalies was provided by the Program Office.

3.1.1 Metric

Site coverage is defined as the fraction of the assigned anomalies surveyed by the TEMTADS.

3.1.2 Data Requirements

The collected data are compared to the original anomaly list. All interferences are noted in the field log book.

3.1.3 Success Criteria

The objective is considered met if 100% of the assigned anomalies are surveyed with the exception of areas that can not be surveyed due to topology / vegetation interferences.

3.2 OBJECTIVE: CALIBRATION STRIP RESULTS

This objective supports that each sensor system is in good working order and collecting physically valid data each day. The calibration strip was surveyed twice daily. The peak positive response of each emplaced item from each run was compared to the physics-based response curves generated prior to data collection on site using each item of interest.

3.2.1 Metric

The reproducibility of the measured response of each sensor system to the items of interest and the comparison of the response to the response predicted by the physics-based model defines this metric.

3.2.2 Data Requirements

Response curves for each sensor / item of interest pair are used to document what the physics-based response of the system to the item should be. The tabulated peak response values from each survey of the Calibration Strip demonstrations the reproducibility and validity of the sensor readings.

3.2.3 Success Criteria

The objective will be considered met if all measured responses fall within the range of physically possible values based on the appropriate response curve. Additionally, the RMS variation in responses should be less than 15% of the measured response and the down-track location of the anomaly should be within 25 cm of the corresponding seeded item's true location.

3.3 OBJECTIVE: LOCATION ACCURACY

An important measure of how efficiently any required remediation will proceed is the accuracy of the predicted location of the targets marked to be dug. Large location errors lead to confusion

among the UXO technicians assigned to the remediation, costing time and often leading to removal of a small, shallow object when a larger, deeper object was the intended target.

3.3.1 Metric

The average error and standard deviation in both horizontal axes will be computed for the items selected for excavation during the validation phase of the study.

3.3.2 Data Requirements

The anomaly fit parameters and the ground truth for the excavated items is required to determine the performance of the fitting routines in terms of the location accuracy.

3.3.3 Success Criteria

This objective is considered as met if the average error in position for both Easting and Northing quantities is less than 5 cm and the standard deviation for both is less than 10 cm.

3.4 OBJECTIVE: DEPTH ACCURACY

An important measure of how efficiently any required remediation will proceed is the accuracy of the predicted depth of the targets marked to be dug. Large depth errors lead to confusion among the UXO technicians assigned to the remediation, costing time and often leading to removal of a small, shallow object when a larger, deeper object was the intended target.

3.4.1 Metric

The standard deviation of the predicted depths with respect to the ground truth is computed for the items which are selected for excavation during the validation phase of the study.

3.4.2 Data Requirements

The anomaly fit parameters and the ground truth for the excavated items are required to determine the performance of the fitting routines in terms of the predicted depth accuracy.

3.4.3 Success Criteria

This objective is considered as met if the average error in depth is less than 5 cm and the standard deviation is less than 10 cm.

3.5 OBJECTIVE: PRODUCTION RATE

This objective considers a major cost driver for the collection of high-density, high-quality geophysical data, the production rate. The faster high quality data can be collected, the higher the financial return on the data collection effort.

3.5.1 Metric

The number of anomalies investigated per day determines the production rate for a cued survey system.

3.5.2 Data Requirements

The metric can be determined from the combination of the field logs and the survey results. The field logs require the amount of time per day spent acquiring the data and the survey results determine the number of anomalies investigated in that time period.

3.5.3 Success Criteria

This objective is considered met if the average production rate is at least 125 anomalies / day.

3.6 OBJECTIVE: DATA THROUGHPUT

The collection of a complete, high-quality data set with the sensor platform is critical to the downstream success of the UXO Classification Study. This objective considers one of the key data quality issues, the ability of the data analysis workflow to support the data collection effort in a timely fashion. To maximize the efficient collection of high quality data, a series of MTADS standard data quality check are conducted during and immediately after data collection on site. Data which pass the QC screen are then processed into archival data stores. Individual anomaly analyses are then conducted on those archival data stores. The data QC / preprocessing portion of the workflow needs to keep pace with the data collection effort for best performance.

3.6.1 Metric

The throughput of the data quality control workflow is at least as fast as the data collection process, providing real time feedback to the data collection team of any issues.

3.6.2 Data Requirements

The data analyst's log books will provide the necessary data for determining the success of this metric.

3.6.3 Success Criteria

This objective is considered met if all collected data can be processed through the data quality control portion of the workflow in a timely fashion.

3.7 OBJECTIVE: RELIABILITY AND ROBUSTNESS

This objective represents an opportunity for all parties involved in the data collection process, especially the vehicle operator, to provide feedback on areas where the process could be improved.

3.7.1 Data Requirements

The data requirements include verbal discussions, communications, and opinions of the entire field team.

4.0 SITE DESCRIPTION

Please refer to the ESTCP UXO Classification Study Demonstration Plan and the MTADS Magnetometer / EM61 MKII Demonstration Plan.

5.0 TEST DESIGN

5.1 CONCEPTUAL EXPERIMENTAL DESIGN

The demonstration was executed in two stages during May and June 2009. The first stage was to characterize the TEMTADS sensor array being demonstrated with respect to the items of interest and to the site specific geology. Pit measurements at various depths and orientations of example articles of each item of interest were made for the munitions of interest and bounding response curves generated. The background response of the demonstration site, as measured by the TEMTADS, was characterized prior to data collection.

The second stage of the demonstration was a survey of the demonstration site using the TEMTADS. The array was positioned roughly over the center of each anomaly on the source anomaly list and a data set collected. Each data set was then inverted using the data analysis methodology discussed in Section 6.0, and estimated target parameters determined. The results and the archive data were submitted to the Program Office along with this report.

5.2 SITE PREPARATION

Please refer to the ESTCP UXO Classification Study Demonstration Plan.

5.3 SYSTEMS SPECIFICATION

This demonstration was conducted using the NRL MTADS tow vehicle and subsystems. The tow vehicle and each subsystem are described further in the following sections.

5.3.1 MTADS Tow Vehicle

The MTADS has been developed with support from ESTCP. The MTADS hardware consists of a low-magnetic-signature vehicle that is used to tow the different sensor arrays over large areas (10 - 25 acres / day) to detect buried UXO. The MTADS tow vehicle and magnetometer array are shown in Figure 5-1.

Figure 5-1 – MTADS tow vehicle and magnetometer array.

5.3.2 RTK GPS System

Positioning is provided using cm-level Real Time Kinematic (RTK) Global Positioning System (GPS) receivers. To achieve cm-level precision, a fixed reference base station is placed on an established first-order survey control point near the survey area. The base station transmits corrections to the GPS rover at 1 Hz via a radio link (450 MHz). The TEMTADS array is located in three-dimensional space using a three-receiver RTK GPS system shown schematically in Figure 2-5 [6]. The three-receiver configuration extends the concept of RTK operations from that of a fixed base station and a moving rover to moving base stations and moving rovers. The lead GPS antenna (and receiver, Main) receives corrections from the fixed base station. This corrected position is reported at 10-20 Hz using a vendor-specific NMEA-0183 message format (PTNL, GGK or GGK). The Main receiver also operates as a 'moving base,' transmitting corrections (by serial cable) to the next GPS receiver (AVR1) which uses the corrections to operate in RTK mode.

A vector (AVR1, heading (yaw), angle (pitch), and range) between the two antennae is reported at 10 Hz using a vendor-specific NMEA-0183 message format (PTNL, AVR or AVR). AVR1 also provides 'moving base' corrections to the third GPS antenna (AVR2) and a second vector (AVR2) is reported at 10 Hz. All GPS measurements are recorded at full RTK precision, ~2-5 cm. For survey-mode arrays, all sensor readings are typically referenced to the GPS 1-PPS pulse output to fully take advantage of the precision of the GPS measurements. In this case of a cued survey, it is not necessary to address these timing issues. For the cued-mode survey, the GPS position is averaged for 2 seconds as part of the data acquisition cycle. The averaged position and orientation information are then recorded to the position (.gps, ASCII format) data file. The details of the file format are provided in Appendix B.

5.3.3 Time-Domain Electromagnetic Sensor

The TEMTADS Array is a 5 x 5 square array of individual sensors. Each sensor has dimensions of 40 cm x 40 cm, for an array of 2 m x 2 m overall dimensions. The rational of this array design

is discussed in Reference 7. The result is a cross-track and down-track separation of 40 cm. Sensor numbering is indicated in Figure 2-5. The transmitter electronics and the data acquisition computer are mounted in the tow vehicle. Custom software written by NRL provides both navigation to the individual anomalies and data acquisition functionality. After the array is positioned roughly centered over the center of the anomaly, the data acquisition cycle is initiated. Each transmitter is fired in a sequence winding outward clockwise from the center position (12). The received signal is recorded for all 25 Rx coils for each transmit cycle. The transmit pulse waveform duration is 2.7s (0.9s block time, 9 repeats within a block, 3 blocks stacked, with a 50% duty cycle). While it is possible to record the entire decay transient at 500 MHz, we have found that binning the data into 115 time gates simplifies the analysis and provides additional signal averaging without significant loss of temporal resolution in the transient decays as discussed in Section 2.1.1 [8]. The data are recorded in a binary format as a single file with 25 data points (one data point per Tx cycle). The filename corresponds to the anomaly ID from the target list under investigation.

5.4 CALIBRATION ACTIVITIES

5.4.1 TEMTADS Sensor Calibration

For the TEMTADS, a significant amount of data has been collected with the system as configured at our Blossom Point facility, both on a test stand and in the towed configuration on our test field [9] and during our recent demonstration at APG [5]. These data and the corresponding fit parameters provide us with a set of reference parameters including those of clear background (i.e. no anomaly present).

Daily calibration efforts will consist of collecting background (no anomaly) data sets at the beginning and end of each survey day and periodically throughout the day at quiet spots identified during the survey setup to determine the system noise floor. A canonical reference object, such as a 4” Al sphere, will also be measured daily to monitor the variation in the system response. Variations should be within 15% of the reference values. These two types of measurements will constitute the daily calibration activities.

5.4.2 Emplaced Sensor Calibration Items

A calibration strip comprised of two replicates of each item of interest was emplaced on site to verify proper system operation on a daily basis. The calibration strip was surveyed each morning and each evening that data were collected. The data were preprocessed, checked for data quality, and then the signal strengths and noise levels compared to the site-specific response curves and background levels to verify consistency of system performance. Please refer to the ESTCP UXO Classification Study Demonstration Plan and the MTADS Magnetometer / EM61 MKII Demonstration Plan for further details.

5.5 DATA COLLECTION PROCEDURES

5.5.1 Scale of Demonstration

We conducted a cued discrimination survey within the 11.8 acre final demonstration site at the Former Camp SLO, CA FUDS of up to 1,500 previously-identified anomalies from the anomaly list generated from the MTADS EM61 MkII data set. This survey was conducted using the NRL TEMTADS. Characterization of the system responses to the items of interest was determined using on site measurements. The data segment (chip) for each anomaly was analyzed, and dipole model fit parameters extracted.

5.5.2 Sample Density

The EMI data spacing for the TEMTADS is fixed at 40 cm in both directions by the array design.

5.5.3 Quality Checks

Preventative maintenance inspections were conducted at least once a day by all team members, focusing particularly on the tow vehicle and sensor trailer. Parts, tools, and materials for many maintenance scenarios are available in the system spares inventory which was on site. Status on any break-downs or failures which resulted in significant delays in operations was immediately reported to the ESTCP Program Office.

Because the TEMTADS operates in a cued mode, the data QC procedures and checks differ from the survey mode instruments. The status of the RTK GPS system can be visually determined by the operator prior to starting the data collection cycle, assuring that the position and orientation information are valid, typical Fix Quality (FQ) 3, during the collection period. A Fix Quality (FQ) value of 3 (RTK Fixed) is the best accuracy (typically 3-5 cm or better). A FQ value of 2 (RTK Float) indicates that the highest level of RTK has not be reached yet and location accuracy can be degraded to as poor as ~1 m. FQs 1 & 4 correspond to the Autonomous and DGPS operational modes, respectively. Data collected under FQ 3 and FQ 2 (at the discretion of the data analyst) are retained.

Two data quality checks were performed on the TEMTADS data. After background subtraction, we made contour plots of the signal at 0.04 ms from the 25 transmit/receive pairs. The plots were visually inspected to verify that there is a well defined anomaly without extraneous signals or dropouts. QC on the transmit/receive cross terms was based on the dipole inversion results. Our experience has been that data glitches show up as reduced dipole fit coherence.

Any data set which has been deemed unsatisfactory by the data analyst was flagged and not processed further. The anomaly corresponding to the flagged data was logged for future re-acquisition. Data which meet these standards are of the quality typical of the TEMTADS system.

5.5.4 Data Handling

Data are stored electronically as collected on the MTADS vehicle data acquisition computer hard drives. Approximately every two survey hours, the collected data were copied onto removable media and transferred to the data analyst for QC/analysis. The data were moved onto the data analyst's computer and the media recycled. Raw data and analysis results were backed up from the data analyst's computer to optical media (CD-R or DVD-R) or external hard disks once daily at a minimum. These results were archived on an internal file server at NRL or SAIC at the end of the survey. Examples of the TEMTADS file formats are provided in Appendix B. All field notes / activity logs were written in ink and stored in archival laboratory notebooks. These notebooks are archived at NRL or SAIC. Relevant sections are reproduced in demonstration reports. Dr. Tom Bell is the POC for obtaining data and other information. His contact information is provided in Appendix A of this report.

5.6 VALIDATION

At the conclusion of data collection activities, all anomalies on the master anomaly list assembled by the Program Office will be excavated. Each item encountered will be identified, photographed, its depth measured, its location determined using cm-level GPS, and the item removed if possible. All non-hazardous items will be saved for later in-air measurements as appropriate. This ground truth information, once released, will be used to validate the objectives listed in Section 3.0

6.0 DATA ANALYSIS PLAN

6.1 PREPROCESSING

The TEMTADS array has 25 transmitters/receiver pairs. For each transmit pulse, we record the response at all of the receivers. Hence, for each target we have a 25 x 25 x N data array, where N is the number of recorded time gates. Normally we use 121 logarithmically spaced gates. In preprocessing, the recorded signals are normalized by the transmitter currents to account for any transmitter variations. We subtract 0.028 ms from the nominal gate times to account for time delay due to effects of the receive coil and electronics [10]. The delay was determined empirically by comparing measured responses for test spheres with theory. Measured responses include distortions due to transmitter ringing and related artifacts out to about 0.040 msec. Consequently we only include response beyond 0.040 ms in our analysis. This leaves 115 gates spaced logarithmically between 0.040 ms and 25 ms.

The background response is subtracted from each target measurement using data collected in a nearby target-free region. Background locations were selected during the initial survey setup. We inter-compared all of the background measurements to evaluate background variability and identified outliers which may correspond to measurements over non-ferrous targets. We did not observe significant background variability at our Blossom Point test site, and were able to use

blank ground measurements from 100 meters away for background subtraction on targets in the test field.

Geo-referencing of the array data is based on the GPS data, which gives the location of the center of the array and the orientation of the array. Sensor locations within the array are fixed by the array geometry. Dipole inversion of the array data (Section 6.2) determines target location in local array-based coordinates. This was transformed to absolute coordinates using the array location and orientation determined from the corresponding GPS data.

6.2 PARAMETER ESTIMATION

The raw signature data from the TEMTADS Array reflect details of the sensor/target geometry as well as inherent EMI response characteristics of the targets themselves. In order to separate out the intrinsic target response properties from sensor/target geometry effects we invert the signature data to estimate principal axis magnetic polarizabilities for the targets. The TEMTADS data are inverted using the standard induced dipole response model wherein the effect of eddy currents set up in the target by the primary field is represented by a set of three orthogonal magnetic dipoles at the target location [11]. The measured signal is a linear function of the induced dipole moment **m**, which can be expressed in terms of a time dependent polarizability tensor **B** as

$$\mathbf{m} = \mathbf{UBU}^{T} \cdot \mathbf{H}_0$$

where **U** is the transformation matrix between the physical coordinate directions and the principal axes of the target and $\mathbf{H}_0$ is the primary field strength at the target. The eigenvalues $\beta_i(t)$ of the polarizability tensor are the principal axis polarizabilities.

Given a set of measurements of the target response with varying geometries or "look angles" at the target, the data can be inverted to determine the (X, Y, Z) location of the target, the orientation of its principal axes (ϕ, θ, ψ), and the principal axis polarizabilities (β_1, β_2, β_3). The basic idea is to search out the set of nine parameters (X, Y, Z, ϕ, θ, ψ, β_1, β_2, β_3) that minimizes the difference between the measured responses and those calculated using the dipole response model.

For the TEMTADS array data, inversion is accomplished by a two-stage method. In the first stage, the target's (X, Y, Z) dipole location is solved for non-linearly. At each iteration within this inversion, the nine element polarizability tensor (**B**) is solved linearly. We require that this tensor be symmetric; therefore, only six elements are unique. Initial guesses for X and Y are determined by a signal-weighted mean. The routine normally loops over a number of initial guesses in Z, keeping the result giving the best fit as measured by the chi-squared value. The non-linear inversion is done simultaneously over all time gates, such that the dipole (X, Y, Z) location applies to all decay times. At each time gate, the eigenvalues and angles are extracted from the polarizability tensor.

In the second stage, six parameters are used: the three spatial parameters (X, Y, Z) and three angles representing the yaw, pitch, and roll of the target (Euler angles ϕ, θ, ψ). Here the eigenvalues of the polarizability tensor are solved for linearly within the 6-parameter non-linear inversion. In this second stage both the target location and its orientation are required to remain constant over all time gates. The value of the best fit X, Y, and Z from the first stage, and the median value of the first-stage angles are used as an initial guess for this stage. Additional loops over depth and angles are included to better ensure finding the global minimum.

Figure 6-1 shows an example of the principal axis polarizabilities determined from TEMTADS array data. The target, a mortar fragment, is a slightly bent plate about ½ cm thick, 25 cm long, and 15 cm wide. The red curve is the polarizability when the primary field is normal to the surface of the plate, while the green and blue curves correspond to cases where the primary field is aligned along each of the edges.

Not every target on the target list will have a strong enough TEM response to support extraction of target polarizabilities. All of the data were run through the inversion routines, and the results manually screened to identify those targets that cannot be reliably parameterized. Several criteria were used in this process: signal strength relative to background, dipole fit error (difference between data and model fit to data), and the visual appearance of the polarizability curves.

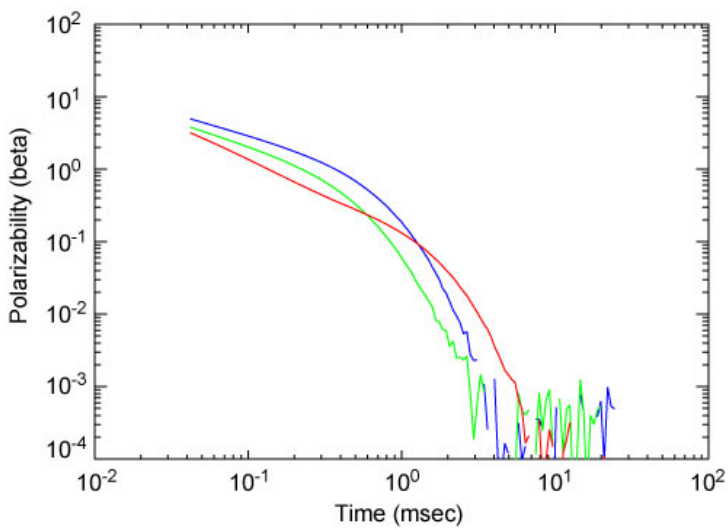

Figure 6-1 – Principal axis polarizabilities for a ½ cm thick by 25cm long by 15cm wide mortar fragment.

6.3 DATA PRODUCT SPECIFICATIONS

See Appendix B for the detailed data product specifications.

7.0 PERFORMANCE RESULTS

The performance objectives for the demonstration were presented in Table 3-1, and are repeated here as Table 7-2 with an additional column indicating whether or not success was achieved.

Prior to our demonstration run at the former Camp SLO, we obtained measurements of each of the four munitions types. Using the derived polarizabilities from these measurements and the forward model of our TEMTADS code, response curves were generated for each munition. These curves plot the minimum expected peak signal (the peak signal when the target is oriented horizontally) and the maximum expected peak (the peak signal when the target is oriented horizontally) from each target as a function of distance below sensor or depth below ground. The peak signal is that obtained from the monostatic term of the center element of the array at the first timegate.

A calibration strip, comprised of two samples of each of the four targets of interest plus two shotputs (Table 7-1), was emplaced on site as a means of verifying proper system operation on a daily basis. The strip was surveyed twice daily, once at the beginning of the day, and once at the end. The sole exception to this procedure occurred on our third day, when brake problems with the vehicle forced an early cessation of activities.

Table 7-1 – Details of Former Camp SLO Calibration Strip

Item ID	**Description**	**Easting (m)**	**Northing (m)**	**Depth (m)**	**Inclination**	**Azimuth (°cw from N)**
T-001	shotput	705,417.00	3,913,682.00	0.25	N/A	N/A
T-002	81mm	705,420.92	3,913,687.63	0.30	Vertical Down	0
T-003	81mm	705,424.10	3,913,692.95	0.30	Horizontal	120
T-004	60mm	705,427.53	3,913,698.54	0.30	Vertical Down	0
T-005	60mm	705,430.85	3,913,704.10	0.30	Horizontal	120
T-006	4.2” mortar	705,434.54	3,913,709.44	0.30	Vertical Down	0
T-007	4.2” mortar	705,437.99	3,913,715.04	0.30	Horizontal	120
T-008	2.36” rocket	705,441.46	3,913,720.24	0.30	Vertical Down	0
T-009	2.36” rocket	705,445.00	3,913,725.91	0.30	Horizontal	120
T-010	shotput	705,448.50	3,913,731.50	0.35	N/A	N/A

Table 7-2 – Performance Objectives for This Demonstration

Performance Objective	Metric	Data Required	Success Criteria	Success?
Site Coverage	Fraction of assigned anomalies interrogated	Survey results	100% as allowed for by topography / vegetation	Yes
Calibration Strip Results	System response consistently matches physics-based model	• System response curves • Daily calibration strip data	• ≤ 15% rms variation in amplitude • Down-track location ± 25cm • All response values fall within bounding curves	Yes
Location Accuracy	Average error and standard deviation in both axes for interrogated items	• Estimated location from analyses • Ground truth from validation effort	ΔN and $\Delta E < 5$ cm σN and $\sigma E < 10$ cm	?
Depth Accuracy	Standard deviation in depth for interrogated items	• Estimated location from analyses • Ground truth from validation effort	ΔDepth < 5 cm σDepth < 10 cm	?
Production Rate	Number of anomalies investigated each day	• Survey results • Log of field work	125 anomalies/day	Yes
Data Throughput	Throughput of data QC process	Log of analysis work	All data QC'ed on site and at pace with survey	Yes
Reliability and Robustness	General Observations	Team feedback	Field team comes to work smiling	Yes

7.1 OBJECTIVE: SITE COVERAGE

A list of previously identified anomalies was provided by the Program Office.

7.1.1 Metric

Site coverage is defined as the fraction of the assigned anomalies surveyed by the TEMTADS.

7.1.2 Data Requirements

The collected data were compared to the original anomaly list. All interferences were noted in the field log book.

7.1.3 Success Criteria

The objective was considered met if 100% of the assigned anomalies are surveyed with the exception of areas that can not be surveyed due to topology / vegetation interferences.

7.1.4 Results

This objective was successfully met. Of the list provided by the Program Office, all but 5 were measured. Failure to measure these 5 anomalies was due to the presence of rocks which prevented the operator from positioning the TEMTADS over the target.

7.2 OBJECTIVE: CALIBRATION STRIP RESULTS

This objective supports that each sensor system is in good working order and collecting physically valid data each day. The calibration strip was surveyed twice daily. The peak positive response of each emplaced item from each run was compared to the physics-based response curves generated prior to data collection on site using each item of interest.

7.2.1 Metric

The reproducibility of the measured response of each sensor system to the items of interest and the comparison of the response to the response predicted by the physics-based model defines this metric.

7.2.2 Data Requirements

Response curves for each sensor / item of interest pair are used to document what the physics-based response of the system to the item should be. The tabulated peak response values from each survey of the Calibration Strip demonstrations the reproducibility and validity of the sensor readings.

7.2.3 Success Criteria

The objective is considered met if all measured responses fall within the range of physically possible values based on the appropriate response curve. Additionally, the RMS variation in responses should be less than 15% of the measured response and the down-track location of the anomaly should be within 25 cm of the corresponding seeded item's true location.

7.2.4 Results

This objective was successfully met. The measured peak signals for all of the emplaced items are shown in Figure 7-1 thru Figure 7-4. The maximum (red) and minimum (blue) response curves are plotted for all objects except the shotput, which has only one curve due to symmetry. The two curves for the 81-mm and 4.2-in mortar are nearly equal. For self-consistency, we have plotted the measurements at the mean inverted depth, rather than the reported depths. The measured values generally fit well within the bounding curves, with the 4.2-in mortar and shotput results the poorest, with a tendency to underestimate the peak value. Careful examination of the data shows that this is the result of the array not being sufficiently well-centered on the targets. Because the response curves are generated assuming the target is directly below the sensor, any offset in the sensor position will result in the derived peak signal being smaller than that predicted by the curve, as is observed.

Table 7-3 shows the mean and standard deviation in the peak measured signal for all of the emplaced Calibration Strip items. Of the 10 items, three give RMS variations above our stated goal of 15%, with only T-008 being significantly above. This target consistently inverted to a depth of 18.5 cm, and thus showed the largest spatial variation in signal. This, coupled with the array not always being properly centered on the target, explains the larger variation for this object.

Table 7-3– Peak Signals for Calibration Strip Emplaced Items

Item ID	Description	Depth (m)	Mean Signal (mV/Amp)	Std Dev. (mV/Amp,1σ)	Variation (%)
T-001	shotput	0.25	27.44	4.18	15.23
T-002	81mm	0.30	15.46	1.39	8.99
T-003	81mm	0.30	10.96	0.91	8.30
T-004	60mm	0.30	8.74	0.89	10.18
T-005	60mm	0.30	6.73	1.13	16.79
T-006	4.2” mortar	0.30	52.38	5.82	11.11
T-007	4.2” mortar	0.30	41.75	5.25	12.57
T-008	2.36” rocket	0.30	32.70	7.91	24.19
T-009	2.36” rocket	0.30	4.04	0.32	7.92
T-010	shotput	0.35	11.82	1.52	12.86

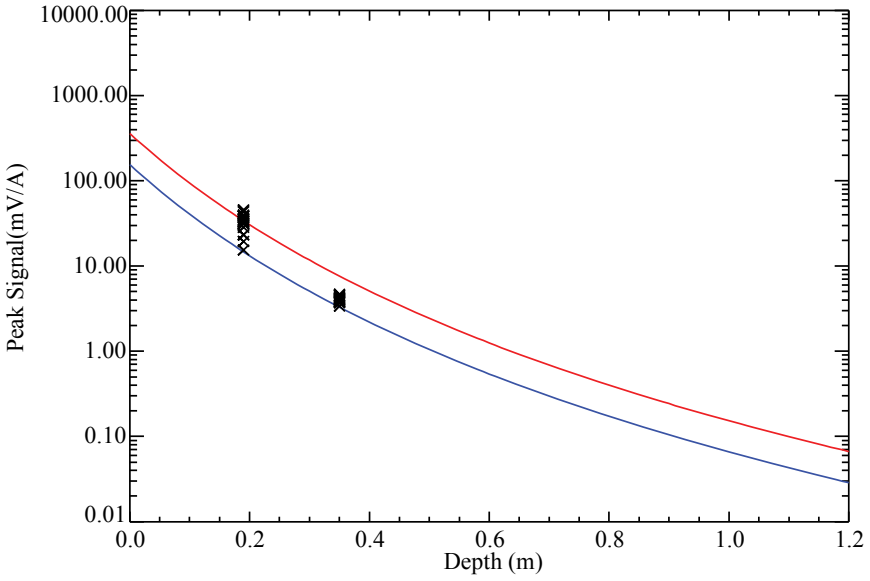

Figure 7-1 – Peak signals compared with response curve for a 2.36-in rocket.

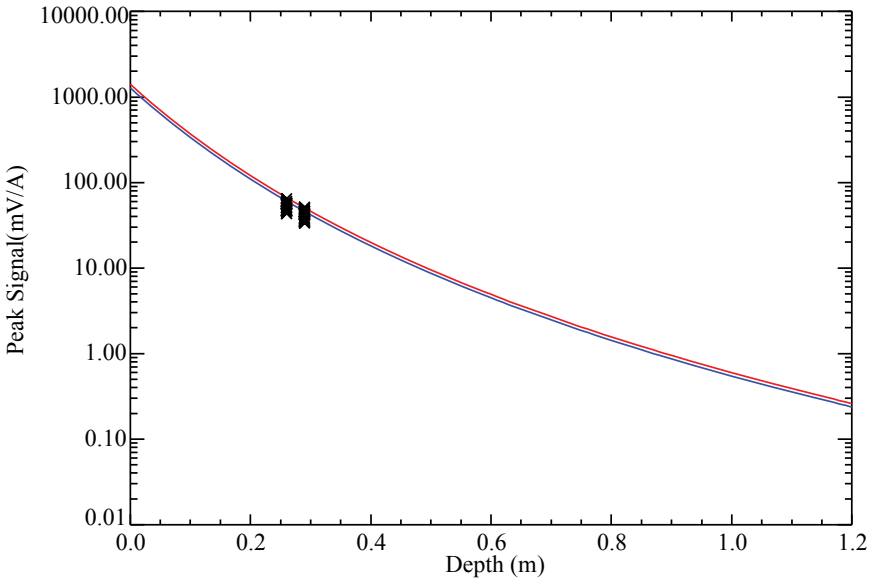

Figure 7-2 – Peak signals compared with response curve for a 4.2-in mortar.

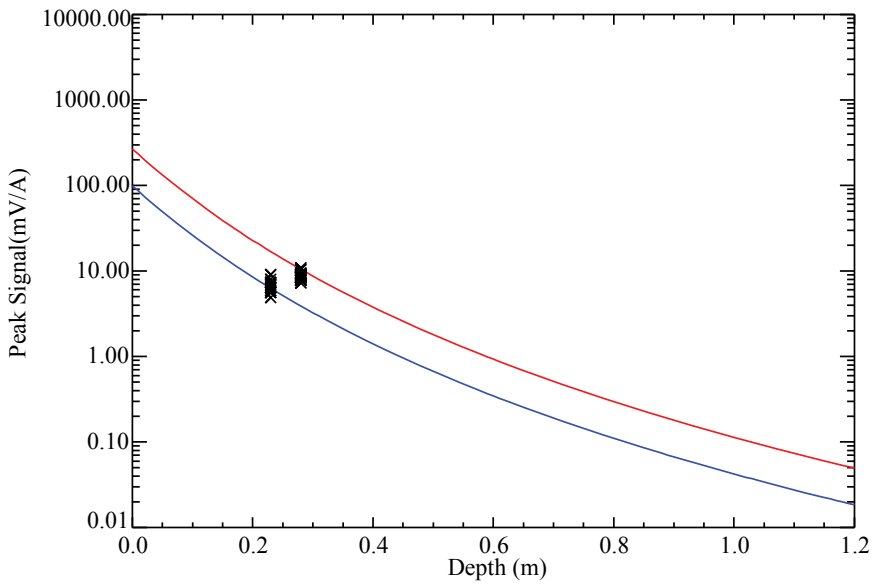

Figure 7-3 – Peak signals compared with response curve for a 60-mm mortar.

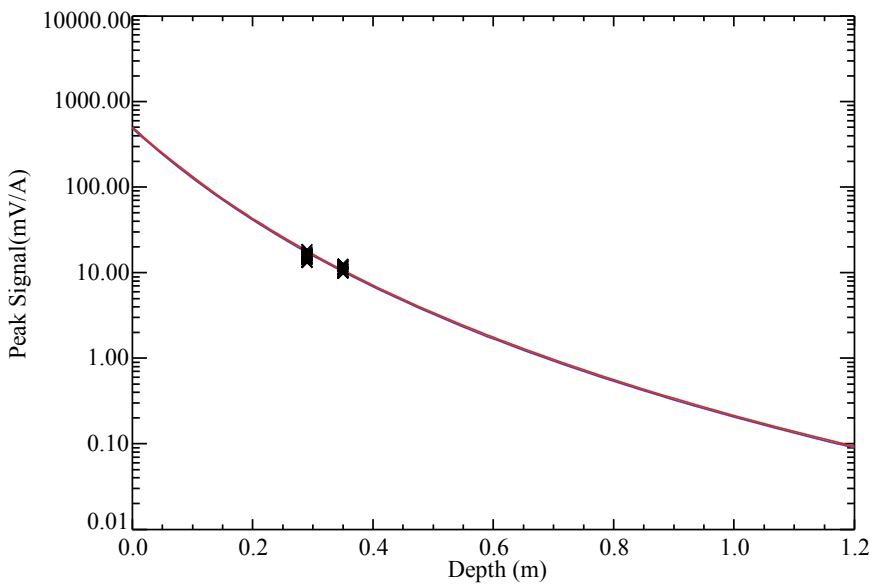

Figure 7-4 – Peak signals compared with response curve for an 81-mm mortar.

The variability and accuracy of the positional fit parameters for the Calibration Strip emplaced items were determined by comparing the inverted Northing and Easting values with reported values. These numbers are shown in Table 7-4. We give the mean vector offset dR between the inverted and reported position as well as the Easting (dx) and Northing (dy) components. The dx and dy values are computed using the inverted positions minus the reported ones.

Two points are clear from the values in Table 7-4. First, the inversion process is very robust, with no standard deviations larger than 2cm. Second, there are a few large discrepancies between our inverted positions and the reported ones. All offsets are below our target value of 25cm, with the exception of T-002. It is possible that some items have drifted or settled since their original emplacement. This matter can be investigated further when the items are recovered during a later phase of the study.

Table 7-4 – Position Accuracy and Variability for Calibration Strip Emplaced Items

Item ID	**Description**	**Depth (m)**	**Mean dR (m)**	**Std Dev dR (m, 1σ)**	**Mean dx (m)**	**Std Dev dx (m)**	**Mean dy (m)**	**Std Dev dy (m)**
T-001	shotput	0.25	0.209	0.007	0.167	0.013	0.124	0.011
T-002	81mm	0.30	0.413	0.008	-0.372	0.008	-0.178	0.010
T-003	81mm	0.30	0.058	0.014	0.028	0.010	-0.049	0.020
T-004	60mm	0.30	0.026	0.013	0.013	0.010	0.015	0.019
T-005	60mm	0.30	0.038	0.012	-0.003	0.011	0.035	0.017
T-006	4.2” mortar	0.30	0.098	0.008	0.082	0.009	0.054	0.009
T-007	4.2” mortar	0.30	0.063	0.008	0.061	0.009	0.013	0.010
T-008	2.36” rocket	0.30	0.035	0.010	-0.027	0.011	0.018	0.011
T-009	2.36” rocket	0.30	0.112	0.016	0.051	0.010	-0.099	0.018
T-010	shotput	0.35	0.166	0.006	0.133	0.008	-0.098	0.014

7.3 OBJECTIVE: LOCATION ACCURACY

An important measure of how efficiently any required remediation will proceed is the accuracy of the predicted location of the targets marked to be dug. Large location errors lead to confusion among the UXO technicians assigned to the remediation, costing time and often leading to removal of a small, shallow object when a larger, deeper object was the intended target.

7.3.1 Metric

The average error and standard deviation in both horizontal axes will be computed for the items selected for excavation during the validation phase of the study.

7.3.2 Data Requirements

The anomaly fit parameters and the ground truth for the excavated items are required to determine the performance of the fitting routines in terms of the location accuracy.

7.3.3 Success Criteria

This objective is considered as met if the average error in position for both Easting and Northing quantities is less than 5 cm and the standard deviation for both is less than 10 cm.

7.3.4 Results

The results necessary to evaluate the success of this metric are not yet available.

7.4 OBJECTIVE: DEPTH ACCURACY

An important measure of how efficiently any required remediation will proceed is the accuracy of the predicted depth of the targets marked to be dug. Large depth errors lead to confusion among the UXO technicians assigned to the remediation, costing time and often leading to removal of a small, shallow object when a larger, deeper object was the intended target.

7.4.1 Metric

The standard deviation of the predicted depths with respect to the ground truth will be computed for the items which are selected for excavation during the validation phase of the study.

7.4.2 Data Requirements

The anomaly fit parameters and the ground truth for the excavated items are required to determine the performance of the fitting routines in terms of the predicted depth accuracy.

7.4.3 Success Criteria

This objective is considered as met if the average error in depth is less than 5 cm and the standard deviation is less than 10 cm.

7.4.4 Results

The results necessary to evaluate the success of this metric are not yet available.

7.5 OBJECTIVE: PRODUCTION RATE

This objective considers a major cost driver for the collection of high-density, high-quality geophysical data, the production rate. The faster high quality data can be collected, the higher the financial return on the data collection effort.

7.5.1 Metric

The number of anomalies investigated per day determines the production rate for a cued survey system.

7.5.2 Data Requirements

The metric can be determined from the combination of the field logs and the survey results. The field logs require the amount of time per day spent acquiring the data and the survey results determine the number of anomalies investigated in that time period.

7.5.3 Success Criteria

This objective is considered met if average production rate is at least 125 anomalies / day.

7.5.4 Results

This objective was successfully met. A total of 1547 anomalies (including redo's) were measured over a 10-day run for an average of 155 anomalies/day. The only days for which our average fell below our goal of 125 anomalies/day were the final day, due to finishing up all targets, and 2 days in which necessary vehicle repairs shortened our workday.

7.6 OBJECTIVE: DATA THROUGHPUT

The collection of a complete, high-quality data set with the sensor platform is critical to the downstream success of the UXO Classification Study. This objective considers one of the key data quality issues, the ability of the data analysis workflow to support the data collection effort in a timely fashion. To maximize the efficient collection of high quality data, a series of MTADS standard data quality check are conducted during and immediately after data collection on site. Data which pass the QC screen are then processed into archival data stores. Individual anomaly analyses were then conducted on those archival data stores. The data QC / preprocessing portion of the workflow needs to keep pace with the data collection effort for best performance.

7.6.1 Metric

The throughput of the data quality control workflow is at least as fast as the data collection process, providing real time feedback to the data collection team of any issues.

7.6.2 Data Requirements

The data analyst's log books will provide the necessary data for determining the success of this metric.

7.6.3 Success Criteria

This objective is considered met if all collected data can be processed through the data quality control portion of the workflow in a timely fashion.

7.6.4 Results

This objective was successfully met. Data were normally downloaded several times during each workday, and quality control on these datasets was usually completed on the same day. Quality control checks successfully caught missed anomalies, a small number of corrupt data files, and targets which needed re-measuring.

7.7 OBJECTIVE: RELIABILITY AND ROBUSTNESS

This objective represents an opportunity for all parties involved in the data collection process, especially the vehicle operator, to provide feedback on areas where the process could be improved.

7.7.1 Data Requirements

This decision was based on verbal discussions, communications, and opinions of the entire field team.

7.7.2 Results

This objective was successfully met. Based on vehicle operator feedback, there were no significant limitations to the efficient use of the system in the field.

8.0 SCHEDULE OF ACTIVITIES

Figure 8-1 gives the overall schedule for the demonstration including deliverables.

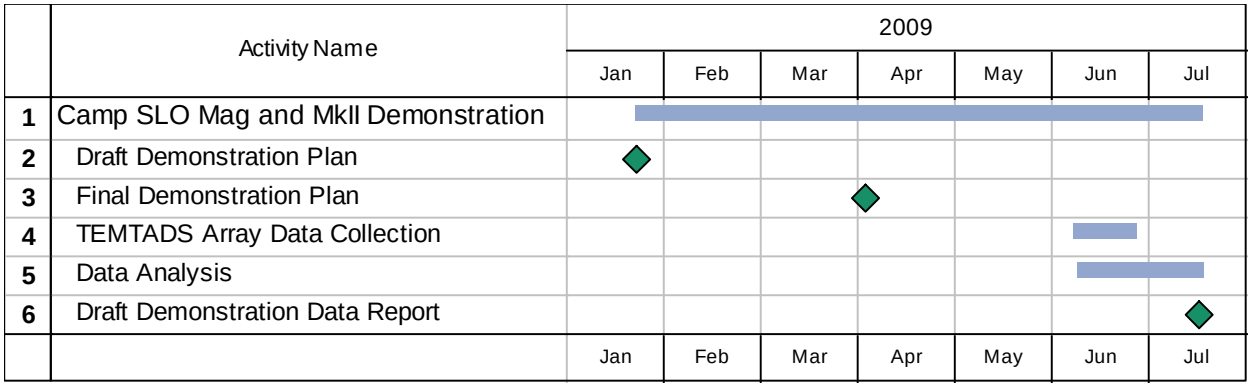

Figure 8-1 – Schedule of all demonstration activities including deliverables.

9.0 MANAGEMENT AND STAFFING

The responsibilities for this demonstration are outlined in Figure 9-1. Dan Steinhurst was the PI of this demonstration and served as the Site and Project Supervisor. Tom Bell served as Quality Assurance Officer. Glenn Harbaugh was the Site Safety Officer and Data Acquisition Operator. Jim Kingdon was the Data Analyst.

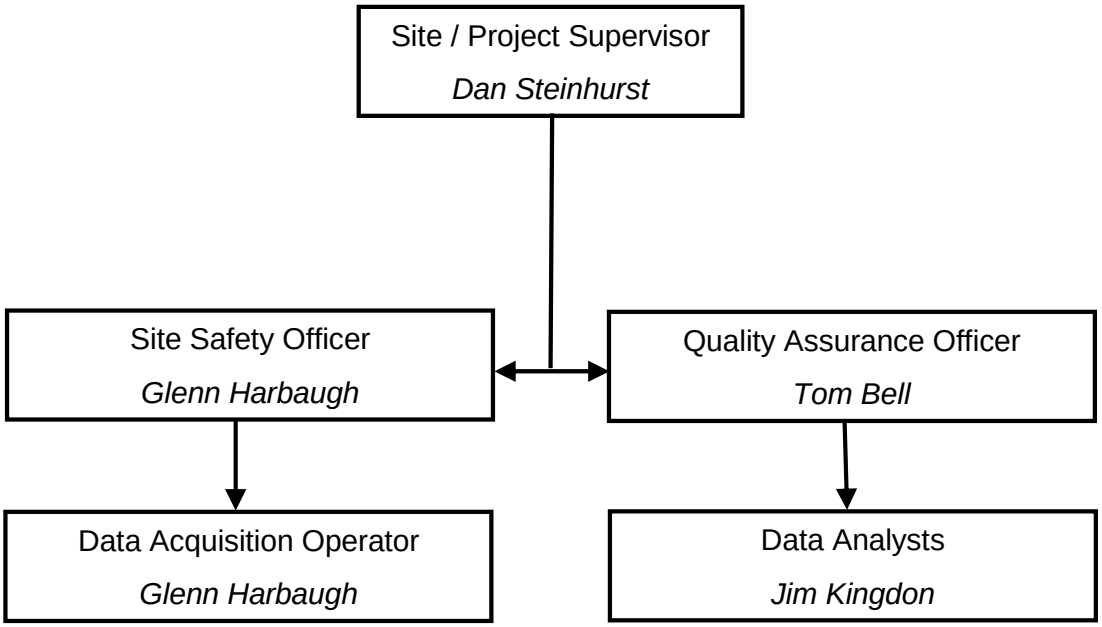

Figure 9-1 – Management and Staffing Wiring Diagram.

10.0 REFERENCES

1. "MTADS Magnetometer / MkII Demonstration Plan, Former Camp San Luis Obispo," D.A. Steinhurst, submitted to ESTCP Program Office, April, 2009.

2. "Enhanced UXO Discrimination Using Frequency-Domain Electromagnetic Induction," ESTCP MM-0033 Final Report, submitted May, 2007.

3. "MTADS Demonstration at Camp Sibert Magnetometer / EM61 MkII / GEM-3 Arrays," Draft Demonstration Data Report, G.R. Harbaugh, D.A. Steinhurst, N. Khadr, August 21, 2008.

4. "Survey of Munitions Response Technologies," ESTCP, ITRC, and SERDP, June, 2006.

5. "STANDARDIZED UXO TECHNOLOGY DEMONSTRATION SITE SCORING RECORD NO. 920 (NRL)," J.S. McClung, ATC-9843, Aberdeen Test Center, MD, November, 2008.

6. Steinhurst, D., Khadr, N., Barrow, B., and Nelson, H. "Moving Platform Orientation for an Unexploded Ordnance Discrimination System," GPS World, 2005, 16/5, 28 – 34.

7. Nelson, H. H., "Array Specification Report," ESTCP MM-0601, June, 2007.

8. Nelson, H. H., ESTCP In-Progress Review, Project MM-0601, March 1, 2007.

9. Nelson, H. H. and Robertson, R., "Design and Construction of the NRL Baseline Ordnance Classification Test Site at Blossom Point," Naval Research Laboratory Memorandum Report NRL/MR/6110—00-8437, March 20, 2000.

10. Bell, T., Barrow, B., Miller, J., and Keiswetter, D., "Time and Frequency Domain Electromagnetic Induction Signatures of Unexploded Ordnance," Subsurface Sensing Technologies and Applications Vol. 2, No. 3, July 2001.

11. Bell, T. H., Barrow, B. J., and Miller, J. T., "Subsurface Discrimination Using Electromagnetic Induction Sensors," IEEE Transactions on Geoscience and Remote Sensing, Vol. 39, No. 6, June 2001.

APPENDIX A. POINTS OF CONTACT

POINT OF CONTACT	ORGANIZATION	Phone Fax e-mail	Role in Project
Dr. Jeff Marqusee	ESTCP Program Office 901 North Stuart Street, Suite 303 Arlington, VA 22203	703-696-2120 (V) 703-696-2114 (F) jeffrey.marqusee@osd.mil	Director, ESTCP
Dr. Anne Andrews	ESTCP Program Office 901 North Stuart Street, Suite 303 Arlington, VA 22203	703-696-3826 (V) 703-696-2114 (F) anne.andrews@osd.mil	Deputy Director, ESTCP
Dr. Herb Nelson	ESTCP Program Office 901 North Stuart Street, Suite 303 Arlington, VA 22203	703-696-8726 (V) 703-696-2114 (F) 202-215-4844 (C) herbert.nelson@osd.mil	Program Manger, MM
Ms. Katherine Kaye	HydroGeoLogic, Inc. 11107 Sunset Hills Road, Suite 400 Reston, VA 20190	410-884-4447 (V) kkaye@hgl.com	Program Manager Assistant, MM
Dr. Dan Steinhurst	Nova Research, Inc. 1900 Elkin St., Ste. 230 Alexandria, VA 22308	202-767-3556 (V) 202-404-8119 (F) 703-850-5217 (C) dan.steinhurst@nrl.navy.mil	PI
Mr. Glenn Harbaugh	Nova Research, Inc. 1900 Elkin St., Ste. 230 Alexandria, VA 22308	301-392-1702 (V) 804-761-5904 (C) glenn.harbaugh.ctr@nrl.navy.mil	Site Safety Officer
Dr. Dean Keiswetter	SAIC 120 Quade Drive Cary NC 27513	919-678-1508 (F) 919-677-1560 (C) dean.a.keiswetter@saic.com	PM - SAIC
Dr. Tom Bell	SAIC 1225 S. Clark Street, Suite 800 Arlington, VA 22202	703-414-3904 (V) thomas.h.bell@saic.com	Quality Assurance Officer
Mr. David Ragsdale	California Polytechnic State University San Luis Obispo, CA 93407	805-756-6662 (V) 805-756-1602 (F) dragsdal@calpoly.edu	Environmental Health & Safety Manager / Risk Management

APPENDIX B. DATA FORMATS

B.1 POSITION / ORIENTATION DATA FILE (*.GPS)

```
Antenna,X_Offset,Y_Offset,Z_Offset,Easting/Yaw,Northing/Pitch,HAE/Range
Main,0.000,1.365,0.730,316256.990,4254211.094,-25.934
AVR1,-0.778,-1.418,0.740,3.40349,0.00761,2.882
AVR2,0.778,-1.418,0.745,1.55718,0.00425,1.554
```

These data files are ASCII format, comma-delimited files. A header line is provided.

Line 1 – Header information

Line 2 – Main GPS antenna data

```
Main              - Antenna Identifier
0.000             - Cross-track distance from array center
1.365             - Down-track distance from array center
0.730             - Vertical distance from array center
316256.990        - Easting (UTM, m) position of Main antenna
4254211.094       - Northing (UTM, m) position of Main antenna
-25.934           - Height-above-ellipsoid (m) position of Main antenna
```

Line 3 & 4 – AVR GPS antenna data (AVR1 as example)

```
AVR1              - Antenna Identifier
-0.778            - Cross-track distance from array center
-1.418            - Down-track distance from array center
0.740             - Vertical distance from array center
3.40349           - Yaw of AVR vector (radians, True North referenced)
0.00761           - Pitch of AVR vector (radians)
2.882             - Range of AVR vector (m)
```

B.2 TEM DATA FILE (*.TEM)

These data files are a binary format generated by a custom .NET serialization routine. They are converted to an ASCII, comma-delimited format in batches as required. Each file contains 25 data points, corresponding to each Tx cycle. Each data point contains the Tx transient and the corresponding 25 Rx transients as a function of time. A pair of header lines is also provided for, one overall file header and one header per data point with the data acquisition parameters. A partial example is provided below.

Line 1 - File Header

```
CPUms,PtNo,LineNo,Delt,BlockT,nRepeats,DtyCyc,nStk,AcqMode,GateWid,Gate
HOff,TxSeq,GateT,TxI_Z,Rx0Z_TxZ,Rx1Z_TxZ,Rx2Z_TxZ,Rx3Z_TxZ,Rx4Z_TxZ,Rx5
Z_TxZ,Rx6Z_TxZ,Rx7Z_TxZ,Rx8Z_TxZ,Rx9Z_TxZ,Rx10Z_TxZ,Rx11Z_TxZ,Rx12Z_TxZ
,Rx13Z_TxZ,Rx14Z_TxZ,Rx15Z_TxZ,Rx16Z_TxZ,Rx17Z_TxZ,Rx18Z_TxZ,Rx19Z_TxZ,
Rx20Z_TxZ,Rx21Z_TxZ,Rx22Z_TxZ,Rx23Z_TxZ,Rx24Z_TxZ,
```

Line 2 - Data Point Header

```
0,1,0,2E-06,0.9,9,0.5,3,2,0.05,5E-05,22,

0           - Start time in ms on CPU clock (always 0)
1           - Data Point Number (always 1)
0           - Line Number (always 0)
2E-06       - Time step for transients (seconds)
0.9         - Base period length (seconds)
9           - Number of Tx cycles in a base period
0.5         - Duty cycle
3           - Number of base periods averaged (or stacked)
2           - Data Acquisition Mode (binned)
0.05        - Gate width as fraction of its own time
5E-05       - Hold-off time (seconds) for first data point
22          - Tx ID number (sensor number + 10)
```

Line 3 - First Data Line in First Data Point

```
,,,,,,,,,,,,2.5E-05,2.01102465120852,-4.71949940100108E-05,-
1.79793904939509E-05,1.39366551389817E-05,-2.55470612811271E-05,-
4.84779418501355E-05,4.05641650778409E-05,6.73185201421361E-06,-
0.000116516308079121,-2.49295973312366E-06,4.21216420108736E-
05,3.70976690069955E-05,-0.000127606649206979,-0.000510366345393333,-
0.000100251591870083,5.19149917311475E-05,3.71239440686929E-05,-
6.05368361143584E-06,-0.000125671808025774,2.44747669528873E-
05,5.7401043406257E-05,-5.14479298585597E-05,-9.42595187481444E-
06,3.27817636140336E-05,-1.1886747308274E-05,-5.57022247620241E-05,
```

B.3 ANOMALY PARAMETER OUTPUT FILE

The fitted parameters for each investigated anomaly are distributed as an Excel 2003 spreadsheet, but an excerpt is given in .csv format below for reference purposes. A header line is provided for information followed by a 116-line block for each anomaly. The first line of each block contains the time gate-independent fit parameters and the remaining 115 contain the time gate-dependent parameters for each anomaly.

```
Anomaly_ID,Anomaly_X,Anomaly_Y,Anomaly_Amplitude,Fit_X,Fit_Y,Fit_Depth(
m),Fit_Phi(deg),Fit_Theta(deg),Fit_Psi(deg),Fit_Coherence,Time_Gate,Bet
a1,Beta2,Beta3

28,402751.00,4369521.75,234.34,402750.926,4369521.686,0.151,250.42,2.02
,76.57,0.99612,,,,
,,,,,,,,,,,1,1.47E+00,1.05E+00,1.08E+00
,,,,,,,,,,,,,,,,,,
,,,,,,,,,,,,,,,,,,
,,,,,,,,,,,,,,,,,,
,,,,,,,,,,,115,2.46E-05,-1.69E-05,-1.60E-04

33,402726.00,4369505.50,15.24,402725.835,4369505.588,0.422,96.25,16.45,
5.26,0.96448,,,,
,,,,,,,,,,,1,1.71E+00,1.23E+00,1.18E+00
,,,,,,,,,,,,,,,,,,
,,,,,,,,,,,,,,,,,,
,,,,,,,,,,,,,,,,,,
,,,,,,,,,,,115,6.56E-04,-1.91E-03,-1.57E-04
```